Citation: Cell Death and Disease (2012) 3, e375; doi:10.1038/cddis.2012.118

www.nature.com/cddis

PP2A-dependent control of transcriptionally active FOXO3a in CD8$^+$ central memory lymphocyte survival requires p47^{phox}

Q Liu[1], L Yi[1], S Sadiq-Ali[1], SM Koontz[1], A Wood[1], N Zhu[1] and SH Jackson*[,1]

Forkhead box O3a (FOXO3a) transcription factor is regulated by complex post-translational modifications that allow for transcriptional control of various apoptosis factors including pro-apoptotic Bim. Although it has been shown that kinases phosphorylate FOXO3a in memory T cells, the role of protein phosphatases in the control of memory T lymphocyte FOXO3a function is less clear. Here, we report that FOXO3a is dephosphorylated (activated) by a protein phosphatase 2A (PP2A)-dependent mechanism in CD8$^+$ memory lymphocytes (Tm) during *Listeria monocytogenes* (*Lm*) infection, which allows for enhanced Bim transcription in nicotinamide adenine dinucleotide phosphate-oxidase p47^{phox}-deficient (p47$^{phox-/-}$) Tm. Consequently, CD8$^+$ Tm from *Lm*-infected p47$^{phox-/-}$ mice express significantly higher levels of each pro-apoptotic Bim protein isoform. Furthermore, there was a profound reduction in the accumulation of CD8$^+$ T central memory (Tcm) cells in infected p47$^{phox-/-}$ spleens, and 65% p47$^{phox-/-}$ mouse moribundity following secondary *Lm* reinfection compared with 25% in wild-type mice. Notably, blocking PP2A activity attenuated FOXO3 activation and Bim transcription in p47$^{phox-/-}$ CD8$^+$ memory lymphocytes. Our findings indicate a critical role for p47^{phox} in a dynamic interplay between PP2A and FOXO3a that regulates pro-apoptotic Bim transcription in CD8$^+$ memory lymphocytes during infection.
Cell Death and Disease (2012) **3,** e375; doi:10.1038/cddis.2012.118; published online 23 August 2012
Subject Category: Immunity

Intracellular bacteria and viruses elicit robust clonal expansion of CD8$^+$ lymphocytes. However, the majority are short-lived effectors (Tec) that undergo programmed cell death after pathogen clearance, while two additional populations of antigen-specific CD8$^+$ lymphocytes are retained as effector memory (Tem) and central memory (Tcm) CD8$^+$ lymphocytes.[1,2] Although surviving memory CD8$^+$ lymphocyte populations remain stable after antigen clearance, memory T lymphocyte (Tm) maintenance is a dynamic process that requires balancing homeostatic proliferation and coordinated Tm apoptosis. Sustaining this balance allows for adequate CD8$^+$ lymphocyte-mediated protective immunity while avoiding the overaccumulation of activated T cells that can predispose to autoimmunity.

Apoptosis is the major mechanism for antigen-specific T lymphocyte attrition post infection, and for controlling Tm homeostasis and turnover. Although both extrinsic and intrinsic apoptosis pathways regulate activated T-cell death *in vitro*, the role of the extrinsic pathway in activated T-cell death *in vivo* remains unresolved.[3,4] In contrast, a dominant role for intrinsic B-cell lymphoma-2 (Bcl-2) family proteins for activated T-cell death and survival has been established.[3,4] It has been shown that specific interactions between, as well as anti and pro-apoptotic Bcl-2 family protein ratios control T-cell survival.[4–6] Bcl-2 is the major anti-apoptotic protein that binds to pro-apoptotic Bim in resting T cells to prevent unstimulated T-cell death.

Recent investigations showed that Bim is critical for activated T-cell contraction in response to super-antigen, and infection with viruses, *Leishmania major*, and *Listeria monocytogenes (Lm)* (reviewed in Kurtulus[4]). In addition, Sabbaugh *et al.*[7] reported that downregulation of Bim is critical for CD8$^+$ memory T-cell survival *in vivo*, and Riou *et al.*[8] reported that reduced Bim expression facilitates CD4$^+$ central memory lymphocyte survival. However, although memory lymphocytes are also activated T lymphocytes, the molecular mechanisms that control memory lymphocyte differentiation and survival are poorly understood.

p47^{phox} is recognized as an adaptor protein for the multi-component nicotinamide adenine dinucleotide phosphate-oxidase (NADPH) oxidase (Nox)2, which mediates the single-electron reduction of oxygen to superoxide anion.[9] Chronic granulomatous disease (CGD) is the genetically inherited immunodeficiency that is caused by defects of structural NADPH oxidase2 (Nox2) proteins.[10] CGD patients are at increased risk of developing life-threatening infection, granulomatous inflammation, and active chronic hyper-inflammatory diseases.[11,12] We reported that T cells express

[1]Molecular Trafficking Unit, Laboratory of Host Defenses, National Institute of Allergy and Infectious Diseases, National Institutes of Health, Bethesda, MD 20892, USA
*Corresponding author: SH Jackson, Molecular Trafficking Unit, Laboratory of Host Defenses, National Institute of Allergy and Infectious Diseases, National Institutes of Health, CRC Building 5-West Labs, Room 5-3942, 10 Center Dr MSC 1456, Bethesda, MD 20892-1456, USA. Tel: 301 435 8040; Fax: 301 480 3549; E-mail: sjackson@niaid.nih.gov
Keywords: forkhead box O3a; protein phosphatase 2A; p47phox; memory T cell
Abbreviations: Nox2, NADPH oxidase 2; CGD, chronic granulomatous disease; *Lm*, *Listeria monocytogenes*; ROS, reactive oxygen species; FOXO3a, forkhead box O3a; PP2A, protein phosphatase 2A; Tcm, central memory T cell; Tem, effector memory T cell; Tec, effector T cell; Tm, memory T cell
Received 12.1.12; revised 23.5.12; accepted 25.5.12; Edited by C Munoz Pinedo

each of the Nox2 structural proteins and that T-cell receptor stimulation induces low-level intracellular Nox2-dependent hydrogen peroxide.[13] Subsequently, we also reported that $p47^{phox}$-deficient ($p47^{phox-/-}$) $CD8^+$ lymphocytes suppress apoptosis *in vivo*,[14] which led us to question how well $p47^{phox-/-}$ $CD8^+$ lymphocytes survive during infection. In this report, we show that in the absence of $p47^{phox}$, antigen-specific $CD8^+$ central memory lymphocyte survival is significantly impaired during *Lm* infection. Our findings demonstrate a novel role for protein phosphatase 2A (PP2A)-dependent forkhead box O3a (FOXO3a) activation, and indicate $p47^{phox}$ is critical in the dynamic interplay between PP2A and FOXO3a that regulates pro-apoptotic Bim transcription in $CD8^+$ memory lymphocytes during infection.

Results

$p47^{phox-/-}$ T lymphocyte responses to primary Lm infection. We reported microenvironment cues within $p47^{phox}$-deficient secondary lymphoid organs suppress $p47^{phox-/-}$ $CD8^+$ lymphocyte death *in vivo*.[14] To further investigate the parameters that constrain $p47^{phox-/-}$ T lymphocyte death, we challenged wild-type (WT) control and $p47^{phox-/-}$ mice[15] with a sub-lethal dose of *Lm* that expresses a truncated ovalbumin protein, rLM-OVA.[16] Although before *Lm* infection the percentages of $CD4^+$ and $CD8^+$ lymphocytes as well as IFNγ expression in $p47^{phox-/-}$ spleens was similar to WT spleens (Supplementary Figure 1), notably, fewer $CD4^+$ and $CD8^+$ T lymphocytes accumulated in *Lm*-infected $p47^{phox-/-}$ spleens than WT spleens, and $p47^{phox-/-}$ lymphocytes secreted significantly less IFNγ than WT lymphocytes during the early phase of *Lm* infection (Figure 1a, Supplementary Figure 2). Importantly, however, we found that $CD8^+$ T lymphocytes from *Lm*-infected $p47^{phox-/-}$ mice lysed target Ova-expressing mouse lymphoma EG7 cells similar to WT lymphocytes on post infection days 3 and 7 (Figure 1b). This indicates that despite the early deficiency of IFNγ secretion, $p47^{phox-/-}$ $CD8^+$ effector cytotoxicity function is intact.

Lm-infected spleens from WT and $p47^{phox-/-}$ mice contained more non-viable T lymphocytes than uninfected control mice 3 days post infection. In addition, *Lm*-infected $p47^{phox-/-}$ spleens contained significantly more ($P<0.001$) non-viable $CD4^+$ and $CD8^+$ T lymphocytes than similarly infected WT spleens on post infection day 3. In additional experiments, we did not detect *Lm*-Ova-specific $CD8^+$ lymphocytes in the LNs or spleens of WT or $p47^{phox-/-}$ mice during the initial 72 h post infection, which indicates this early T lymphocyte death is nonselective and not due to the death of antigen-specific $CD8^+$ lymphocyte. Collectively, these investigations show that relative to WT mice there is more pronounced early T-cell death in *Lm*-infected $p47^{phox-/-}$ spleens. Consequently, few T lymphocytes accumulate in $p47^{phox-/-}$ mice during primary *Lm* infection.

Impaired $p47^{phox-/-}$ mouse $CD8^+$ Tcm responses during Lm infection. To determine whether the observed $p47^{phox-/-}$ $CD8^+$ T lymphocyte loss was mediated by Nox2 enzymatic activity we compared mouse survival, and used flow cytometry to distinguish total and antigen-specific $CD8^+$ lymphocyte differentiation and survival in the *Lm*-infected

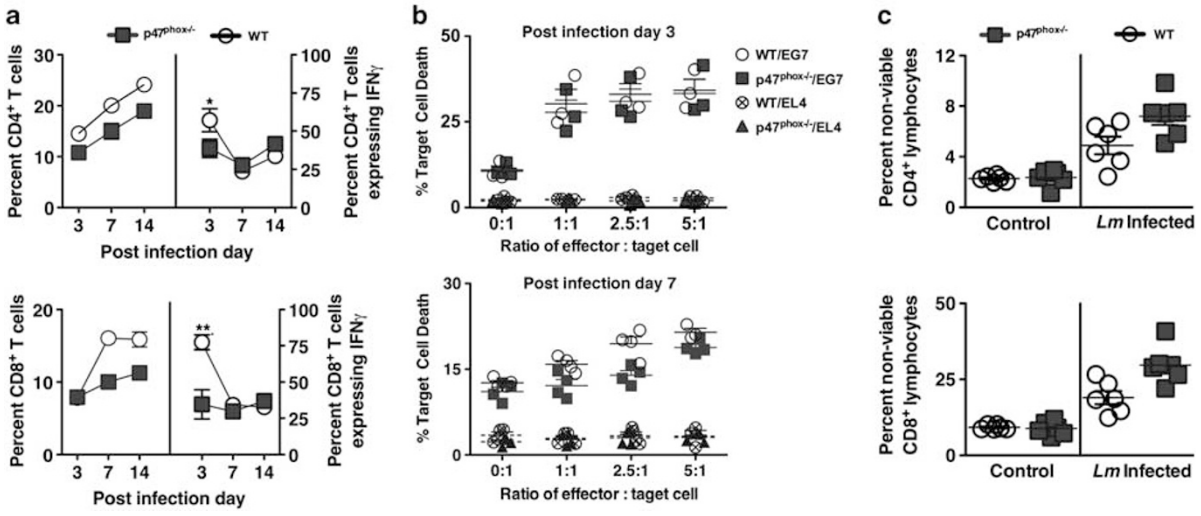

Figure 1 Significantly fewer $CD4^+$ and $CD8^+$ lymphocytes accumulate in the infected spleens of $p47^{phox-/-}$ mice during primary *L. monocytogenes* infection. WT (○) and $p47^{phox-/-}$ (■) mice were infected with 5×10^4 CFU (0.1 LD_{50}) rLM-OVA. On the indicated post infection day the mice were euthanized and single-cell splenocyte cultures were incubated for 3–5 h with 1 μM $OVA_{323-339}$ and/or $OVA_{257-264}$ peptides for CD4 and CD8 T lymphocyte stimulation, respectively. Monensin was added for the final 2 h of culture, and the cells were harvested and stained for surface CD4, CD8, and intracellular IFNγ expression. (**a**) Percentage of $CD4^+$ and $CD8^+$ lymphocytes, and the percentage of $CD4^+$ and $CD8^+$ lymphocytes expressing IFNγ. The data are the mean (± S.E.M.) for six individual mice from two separate experiments with three of each genotype/experiment. (**b**) $p47^{phox-/-}$ $CD8^+$ T lymphocytes effectively kill target cells. On post infection days 3 and 7, as indicated, spleen-derived $CD8^+$ T cells were co-cultured with CFSE-labeled EL4 or E.G7-OVA target cells at the indicated effect: target cell ratios for 4 h. The results are presented as percentage of PI^+ E.G7-OVA or EL4 target cells. Results are the mean (± S.E.M.) of three independent experiments including three of each genotype/experiment. (**c**) On post infection day 3, the percentage of non-viable EMA^+ $CD4^+$ or EMA^+CD8^+ lymphocytes was determined. The data are the mean (± S.E.M.) percentage for five individual mice. $^*P<0.005$, $^{**}P<0.05$

p47$^{phox-/-}$ and Nox2 catalytic gp91^{phox}/Nox2-deficient mice.[17] Interestingly and in sharp contrast to p47$^{phox-/-}$ and WT mice, 25% of gp91$^{phox-/-}$ mice became moribund following primary sub-lethal *Lm* infection (Figure 2a). We also found that fewer total and $Ova_{257-264}$ antigen-specific CD8$^+$ T cells accumulated in p47$^{phox-/-}$ and gp91$^{phox-/-}$ spleens 7 days after infection than similarly treated WT spleens (Figure 2b). However, the total (Figure 2c) and antigen-specific (Figure 2d) CD127^{low}CD62L^{low} effector (Tec) and CD127^{high}CD62L^{low} effector memory (Tem) CD8$^+$ subset[18] responses were exaggerated in both gp91$^{phox-/-}$ and p47$^{phox-/-}$ mice relative to WT mice; albeit more pronounced for p47$^{phox-/-}$ effectors than gp91$^{phox-/-}$ CD8$^+$ effector lymphocytes. Moreover, relative to WT and gp91$^{phox-/-}$ mice, the total accumulation of central memory CD127^{high}CD62L^{high} (Tcm) CD8$^+$ lymphocytes[18] was significantly reduced in *Lm*-infected p47$^{phox-/-}$ spleens (Figure 2c). Correspondingly, there were 4.5 and 3 times more antigen-specific Tcm in *Lm*-infected WT and gp91$^{phox-/-}$ spleens, respectively, than similarly treated p47$^{phox-/-}$ mice (Figure 2d). Thus, unlike WT mice, acute *Lm* infection triggers more antigen-specific Tec and Tem expansion in p47$^{phox-/-}$ and gp91$^{phox-/-}$ mice. However, this effector response is more robust in p47$^{phox-/-phox-/-}$ mice than gp91$^{phox-/-}$ mice. The effector function of both CD8$^+$ effector subset is immediate,[19] which maybe why the p47$^{phox-/-}$ mouse survival is better relative to the gp91$^{phox-/-}$ mice in response to primary *Lm* infection (Figure 2a). In contrast, significantly fewer antigen-specific CD8$^+$ Tcm accumulated in p47$^{phox-/-}$ spleens than WT and gp91$^{phox-/-}$ spleens during primary *Lm* infection, which suggest that the selective expansion of CD8$^+$ Tcm is impaired in p47$^{phox-/-}$ mice. These findings also reveal that the *Lm* elicited peak CD8$^+$ effector lymphocyte response on post infection day 7, and the mounting CD8$^+$ central memory lymphocyte response are distinct in WT and Nox2-reactive oxygen species (ROS)-deficient p47$^{phox-/-}$ and gp91$^{phox-/-}$ mice. However, the data also demonstrate that p47$^{phox-/-}$ and gp91$^{phox-/-phox-/-}$ CD8$^+$ T-cell subset differentiation and expansion are different during *Lm* infection, which suggest that the profound p47$^{phox-/-}$ Tcm death is independent of Nox2 catalytic activity.

CD8$^+$ memory lymphocytes has a pivotal role in the protective immune response against *Lm* reinfection.[20,21] Strikingly, 65% of p47$^{phox-/-}$ mice became moribund within 72 h of reinfection with a 10-fold lethal doses of *Lm,* indicating that the paucity of antigen-specific CD8$^+$ Tcm was disadvantageous for p47$^{phox-/-}$ mice (Figure 2e). In contrast, just 25% of both gp91$^{phox-/-}$ and WT mice became moribund after *Lm* reinfection (Figure 2e), which suggest unlike WT and gp91$^{phox-/-}$ mice, p47$^{phox-/-}$ mice lack sufficient CD8$^+$ Tcm to mount effective T-cell-mediated protection following rechallenge with *Lm*. Collectively, these investigations demonstrate that there is an essential role for p47^{phox} protein rather that Nox2 enzymatic activity for CD8$^+$ Tcm differentiation and survival.

p47$^{phox-/-}$ Tm loss is mediated by Bim. Analyses of antigen-specific CD8$^+$ subset phenotypes in the *Lm*-reinfected WT and p47$^{phox-/-}$ mice revealed there was significant expansion of both WT and p47$^{phox-/-}$ CD8$^+$ Tcm populations (Figure 3). However, similar to the primary infection response, the p47$^{phox-/-}$ antigen-specific Tcm population was still significantly less than WT Tcm 24 h post reinfection (Figure 3a). Furthermore, and consistent with the specific loss of the Tcm population, 10 days post reinfection there was twofold more contraction in the p47$^{phox-/-}$ Tcm subset than WT Tcm (Figure 3b). Additionally, similar to the primary CD8$^+$ response to *Lm*, significantly more effector, Tem and Tec, cells accumulated in the spleens of p47$^{phox-/-}$ mice that survived secondary *Lm* reinfection than similarly treated WT mice (Figures 3a and b).

Our previous investigations revealed p47$^{phox-/-}$ CD8$^+$ lymphocytes have an intrinsic apoptotic pathway defect and that micro-environmental cues suppress pro-apoptotic Bim and PUMA protein expression in inflamed p47$^{phox-/-}$ secondary lymphoid tissues.[14] Using flow cytometry we examined these parameters in *Lm*-infected mice, and observed that nearly twice as many p47$^{phox-/-}$ CD8$^+$ T lymphocytes expressed more of the most potent Bim isoform, Bim short (Bim_s,[22]), than similarly treated WT mice after primary *Lm* infection (Figure 3c). In response to *Lm* reinfection, both WT and p47$^{phox-/-}$ CD8$^+$ Tem and Tcm expressed more Bim_s than Tec (Figure 3d, Supplementary Figure 3). Though as shown in Figure 3d, more p47$^{phox-/-}$ Tcm than Tem expressed Bim_s after *Lm* reinfection, whereas the reverse was found in similarly treated WT mice. Therefore, these studies demonstrate that although p47$^{phox-/-}$ mice mount a proliferative CD8$^+$ memory lymphocyte response to secondary *Lm* infection, Tcm in *Lm*-infected p47$^{phox-/-}$ mice express higher levels of pro-apoptotic Bim than similarly treated WT mice, and ultimately fewer antigen-specific Tcm accumulate in *Lm*-infected p47$^{phox-/-}$ spleens.

In additional experiments we generated memory CD8$^+$ cells, by restimulating *Lm*-infected mouse spleens with $OVA_{257-264}$-peptide, *in vitro*, to allow for antigen-specific T-cell expansion to further examine Bim protein expression and regulation. Flow cytometric analysis of cultured whole spleen populations showed the p47$^{phox-/-}$ cultures yielded significantly fewer total CD8$^+$ and Tcm lymphocytes, but significantly more Tem lymphocytes than WT cultures (Figures 4a–c). In addition, Bim transcription was significantly higher in the *ex vivo*-induced p47$^{phox-/-}$ memory CD8$^+$ cells than similarly treated WT cells (Figure 4d). Likewise, the analysis revealed that the transcription of PUMA was also significantly enhanced in the *ex vivo*-induced p47$^{phox-/-}$ memory CD8$^+$ lymphocytes (Supplementary Figure 4). Immunoblots of protein from the CD8$^+$ lymphocyte isolates also showed enhanced Bim expression in p47$^{phox-/-}$ memory lymphocytes relative to WT cells (Figure 4e). Notably, and in agreement with the flow cytometry analysis of Bim expression (Figure 3c), Bim short is also detectable in p47$^{phox-/-}$ cells in the overexposed immunoblot image in Figure 4e.

It has been shown that Bim protein expression is regulated via an ERK1/2-dependent post-translational modification.[23] Therefore, we used western analysis to assessed this regulation in the *ex vivo*-generated spleen CD8$^+$ memory cells. As shown in Figure 4f, the expression of total and phosphorylated Erk 1/2 were equivalent in *ex vivo*-generated spleen CD8$^+$ memory lymphocytes from WT and p47$^{phox-/-}$

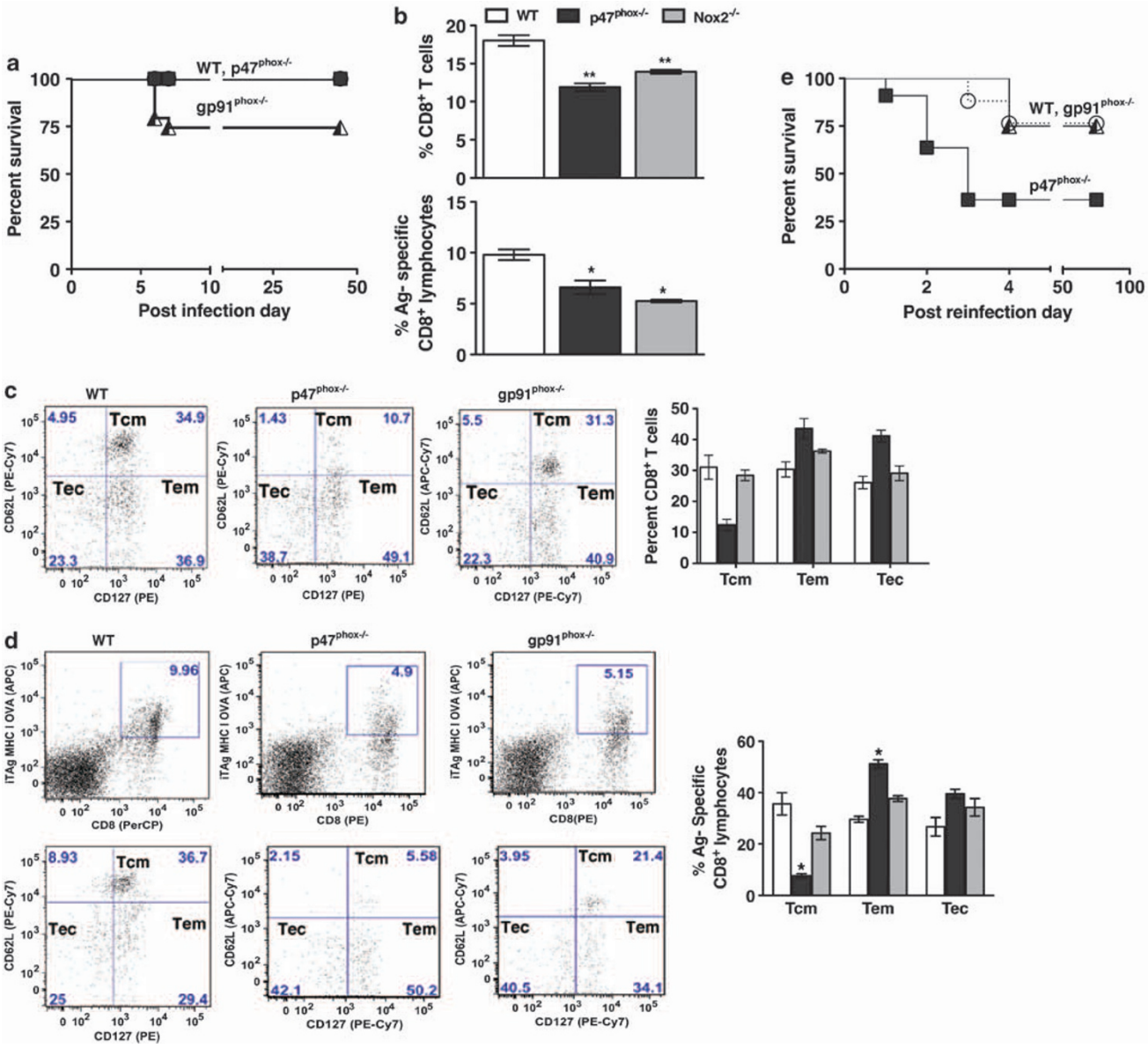

Figure 2 CD8$^+$ Tcm subset is reduced in p47$^{phox-/-}$ mice during *Lm* infection. WT, p47$^{phox-/-}$, and gp91$^{phox-/-}$ mice were infected with 5×10^4 CFU (0.1 LD_{50}) rLM-OVA. (**a**) Survival of WT (○), p47$^{phox-/-}$ (■), and gp91$^{phox-/-}$ (◭) mice, $P<0.001$. On post infection day 7, the mice were euthanized and single-cell splenocyte cultures were incubated for 5 h with 1 μM $OVA_{257-264}$ peptide for CD8$^+$ T lymphocyte stimulation. Monensin was added for the final 2 h of culture, and the cells were harvested and stained for surface CD8, CD127, CD62L, and $OVA_{257-264}$-tetramer expression. (**b**) Percentage of total (top) and $OVA_{257-264}$ antigen-specific (bottom) CD8$^+$ lymphocytes. Percentage of (**c**) total and (**d**) $OVA_{257-264}$ antigen-specific CD8$^+$ lymphocyte effector (Tec) and effector memory (Tem) lymphocytes, and central memory (Tcm) CD8$^+$ T lymphocyte subsets. The data are the mean (± S.E.M.) for six individual mice from two separate experiments with three of each genotype/experiment. *$P<0.001$, **$P<0.05$. Forty-five days post-primary infection WT (□), p47$^{phox-/-}$ (■), and gp91$^{phox-/-}$ (◭) mice were reinfected with 5×10^6 CFU ($10 \times$ LD_{50}) rLM-OVA. (**e**) Survival of WT, p47$^{phox-/-}$, and gp91$^{phox-/-}$ mice, $P<0.01$

mice (Figure 4f), which indicates that the post translational regulation of Bim[23] in p47$^{phox-/-}$ CD8$^+$ memory lymphocytes is comparable to similarly treated WT memory lymphocytes.

p47^{phox} regulates the post translation modification of FOXO3a through PP2A in CD8$^+$ memory lymphocytes to control pro-apoptotic Bim expression. Highly phosphorylated FOXO3a is retained in the cytoplasm and targeted for ubiquination, while unphosphorylated FOXO3a translocates to the nucleus and controls the expression of several apoptosis target genes including Bim and FasL.[24] To further distinguish the regulation of Bim in p47$^{phox-/-}$ CD8$^+$ memory lymphocytes, we used western analysis to assess the signaling intermediaries involved in Bim protein expression. We found elevated levels of total FOXO3a protein in p47$^{phox-/-}$ CD8$^+$ memory lymphocytes relative to similarly treated WT memory lymphocytes (Figure 5a). In addition, the elevated FOXO3a was hypo-phosphorylated in p47$^{phox-/-}$ CD8$^+$ memory lymphocytes relative to WT, which indicates

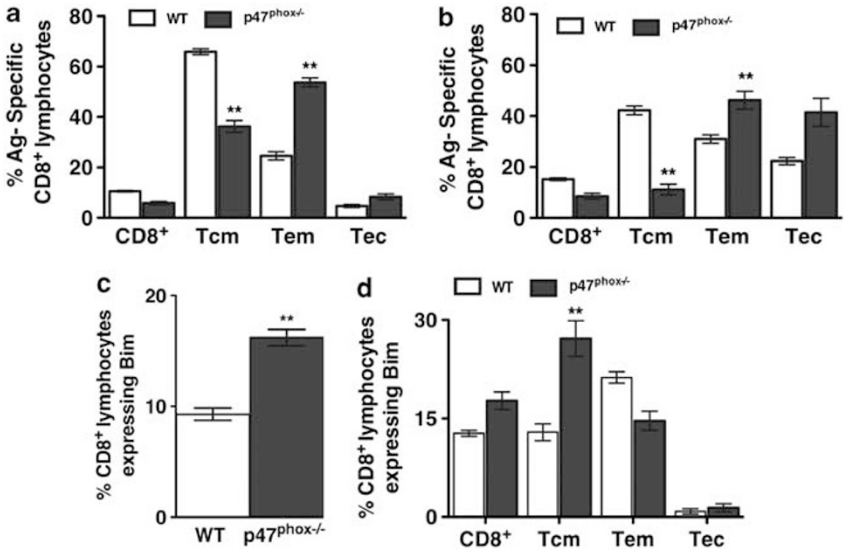

Figure 3 *Lm*-infected p47$^{phox-/-}$ CD8$^+$ memory lymphocytes express more pro-apoptotic Bim protein. Twenty-four hours (**a**) and 10 days (**b**) post reinfection freshly isolated splenocytes from WT and p47$^{phox-/-}$ mice were fixed and stained, and then analyzed for CD8, CD127, CD62L, and $OVA_{257-264}$-tetramer expression. The data are the mean (± S.E.M.) percentage for six individual mice from two separate experiments with three of each genotype/experiment. $^{**}P<0.0001$. Single-cell splenocyte cultures from WT and p47$^{phox-/-}$ mice infected with (**c**) 5×10^4 CFU (0.1 LD_{50}) rLM-OVA, or (**d**) reinfected with 5×10^6 CFU ($10\times$ LD_{50}) for 24 h were fixed and stained, and then analyzed for CD8, CD127, CD62L, and intracellular Bim expression by flow-cytometry. The percentage of CD8$^+$ lymphocytes expressing Bim is shown. The data are the mean (± S.E.M.) percentage for six individual mice from two separate experiments with three of each genotype/experiment $^{**}P<0.005$

that FOXO3a is more transcriptionally active in p47$^{phox-/-}$ CD8$^+$ memory cells, and is consistent with finding that Bim transcription is enhanced in p47$^{phox-/-}$ CD8$^+$ memory lymphocytes (Figure 4d).

Various kinases, including AKT and IKK-β, regulate the transcriptional activity of FOXO3a by direct phosphorylation.[24–26] Furthermore, a recent report by Riou *et al.*[8] showed AKT and IKK-β regulate FOXO3a phosphorylation to attenuate human CD4$^+$ memory T-cell apoptosis. Interestingly, we found that compared with WT CD8$^+$ memory lymphocytes both AKT and IKK-β were hyper-phosphorylated (pIKKα/β (ser176/180) and pAKT (Ser473)/pAKT (Thr308)) in p47$^{phox-/-}$ CD8$^+$ memory lymphocytes (Figures 5b and c), which suggest that the dysregulated FOXO3a activity is not mediated by kinase activity alone in p47$^{phox-/-}$ CD8$^+$ memory lymphocytes. Therefore, we speculated whether the decreased phosphorylation of FOXO3a in p47$^{phox-/-}$ CD8$^+$ memory cells was due to enhanced phosphatase activity. As shown in Figure 5d, p47$^{phox-/-}$ CD8$^+$ memory lymphocytes have more robust PP2A expression than similarly treated WT cells. In additional experiments, we found that using okadaic acid (OA) to selectively inhibit PP2A,[27] enhanced FOXO3a phosphorylation in both p47$^{phox-/-}$ and WT CD8$^+$ memory lymphocytes (Figure 5e), thereby supporting that PP2A also regulates FOXO3a activity in memory lymphocytes. We also found that Bim transcription was reduced by 35% in OA-treated p47$^{phox-/-}$ CD8$^+$ memory lymphocytes (Figure 5f), and that the percentage of non-viable cells in the OA-treated p47$^{phox-/-}$ CD8$^+$ memory lymphocyte cultures was reduced 30% compared with untreated p47$^{phox-/-}$ CD8$^+$ memory lymphocytes (Figure 5g). Collectively, these findings demonstrate that PP2A also regulates FOXO3a activity in CD8$^+$ memory lymphocytes and indicate that p47^{phox} is necessary for regulating PP2A activity. Furthermore, these investigations suggest that the selective expansion of CD8$^+$ Tcm is compromised in p47$^{phox-/-}$ mice during *Lm* infection because in the absence of p47^{phox} FOXO3a is transcriptionally activated by a PP2A-dependent mechanism that allows for unchecked Bim expression.

Discussion

Potent T-cell memory is necessary for protective adaptive immunity. Consequently, understanding the molecular mechanism(s) that control memory T-cell survival and turnover are critically important. Apoptosis decisively regulates memory T-cell homeostasis, and several investigations have shown that limiting pro-apoptotic Bim protein activity is pivotal for memory T-cell survival.[4,7,8] Intensive investigations also have eloquently demonstrated that Bcl-2/Bim balance is critical for memory T-cell development. Furthermore, a recent investigation by Kurtulus *et al.*[28] reinforces that Bcl-2 is a critical anti-apoptotic factor that antagonizes Bim activity, and thereby facilitates memory T-cell survival. However, there are other mechanisms that are also important for regulating Bim that need to be elucidated. In that regard, emerging data from investigations of how Bim expression is regulated has demonstrated that FOXO3a is an essential transcription factor that controls Bim expression in CD4$^+$ memory T cells.[8] In this study we examined the parameters that constrain CD8$^+$ T lymphocyte death during infection in p47$^{phox-/-}$ mice, which we previously showed develop lymphoid hyperplasia in part due to suppressed Bim-mediated apoptosis.[14] In response to *Lm* infection p47$^{phox-/-}$ T lymphocytes showed decreased survival. Notably, there was a profound reduction

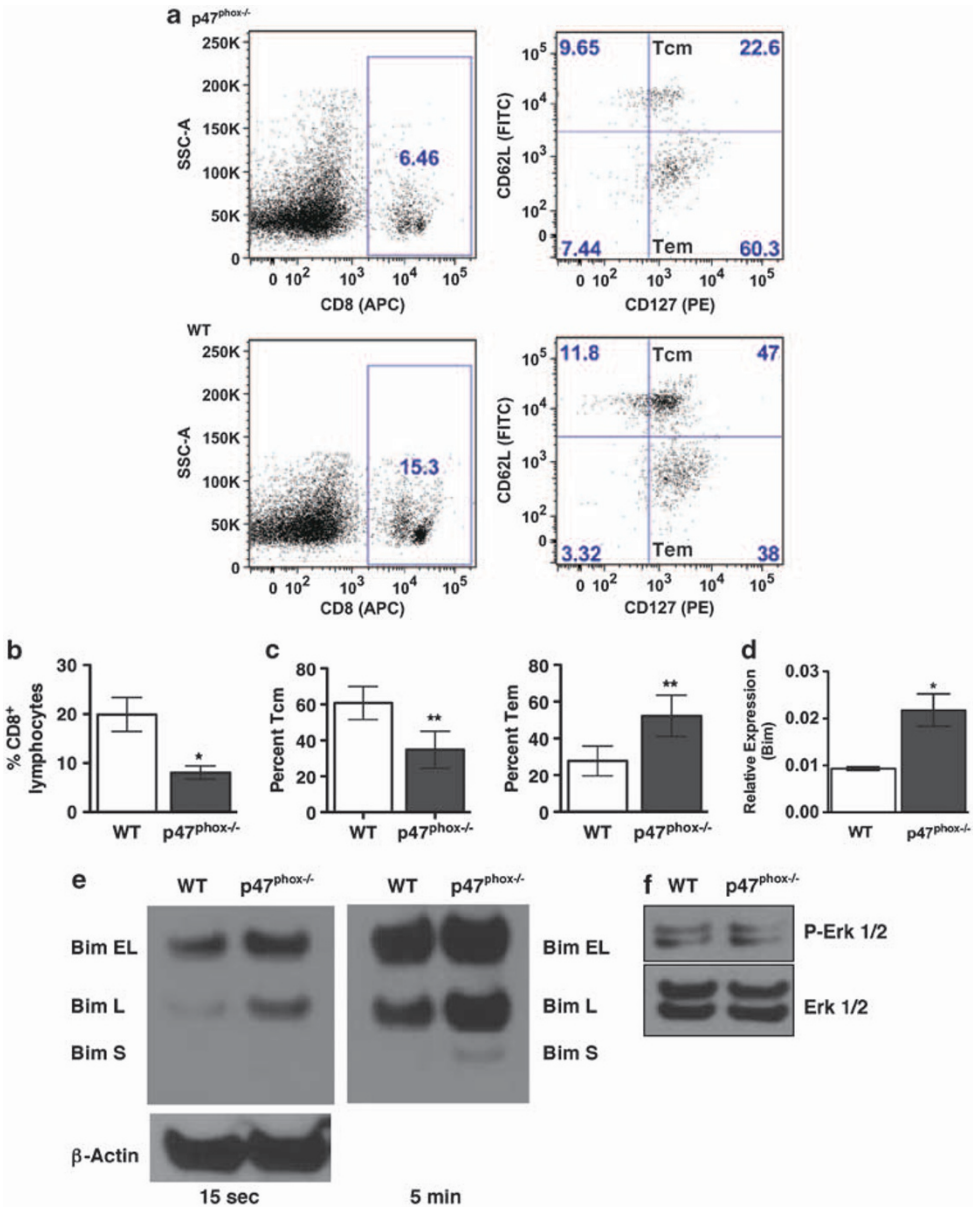

Figure 4 *Ex vivo*-generated $p47^{phox-/-}$ $CD8^+$ memory lymphocytes express more pro-apoptotic Bim protein. Single-cell splenocyte cultures from surviving WT and $p47^{phox-/-}$ mice infected with 5×10^4 CFU (0.1 LD_{50}) rLM-OVA for 45–60 days were restimulated *in vitro* for 2 days with 1 μM $OVA_{257-264}$ peptide. The cells were harvested and stained for surface CD8, CD127, and CD62L. (**a**) Representative ($n = 4$) flow cytometry profile of *ex vivo* $OVA_{257-264}$ peptide stimulated WT and $p47^{phox-/-}$ $CD8^+$ lymphocytes. Percent $CD8^+$ (**b**), and Tem and Tcm lymphocytes (**c**) in *ex vivo* splenocyte cultures. Results are representative of four independent experiments including pooled cells from 8–10 of each genotype/experiment. $^*P \leq 0.02$, $^{**}P < 0.003$. $CD8^+$ lymphocytes were isolated from the *ex vivo* $OVA_{257-264}$ peptide-stimulated splenocyte cultures. (**d**) Real-time PCR quantification of Bim expression. Values are relative to expression of the gene encoding RPS29. $^*P < 0.02$. Total cell lysates from $p47^{phox-/-}$ and WT $CD8^+$ lymphocytes were blotted with (**e**) anti-Bim and (**f**) anti-Erk1/2. Results are representative of three independent experiments including pooled cells from 8–10 of each genotype/experiment

in the accumulation of antigen-specific $CD8^+$ Tcm cells in infected $p47^{phox-/-}$ spleens, and Tcm from secondarily infected $p47^{phox-/-}$ mice expressed significantly higher levels of pro-apoptotic Bim.

Previous investigations demonstrated that the innate immune response to *Lm* infection is impaired in mice lacking Nox2-dependent ROS.[29,30] However, the role of T lymphocyte Nox2 protein-mediated responses in *Lm* infection remains unclear. In this manuscript, we show for what we believe is the first time that $p47^{phox-/-}$ and Nox2 enzyme catalytic subunit $gp91^{phox-/-}$ mice develop distinct T lymphocyte subset responses in response to infection. Specifically, Tcm expansion and differentiation in *Lm*-infected $gp91^{phox-/-}$ mice were comparable to similarly treated WT controls. Furthermore, *Lm* reinfection caused 65% moribundity in $p47^{phox-/-}$ mice unlike $gp91^{phox-/-}$ and WT mice. Therefore, we conclude that the observed survival defect in $p47^{phox-/-}$ $CD8^+$ memory lymphocytes is due to the lack of

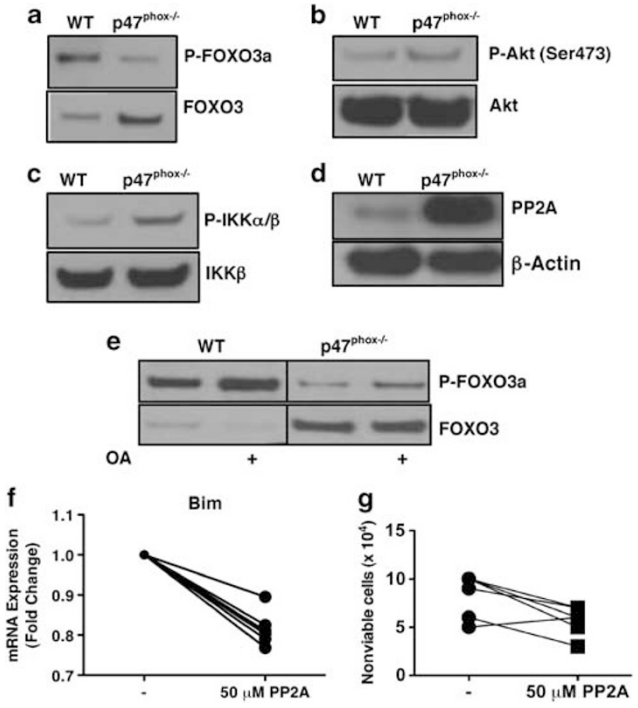

Figure 5 p47^{phox} regulates the post translation modification of FOXO3a through PP2A in CD8$^+$ memory lymphocytes to attenuate pro-apoptotic Bim expression. CD8$^+$ lymphocytes were isolated from the *ex vivo* $OVA_{257-264}$ peptide-stimulated splenocyte cultures described in Figure 4. Total cell lysates from p47$^{phox-/-}$ and WT CD8$^+$ lymphocytes were blotted with phosphorylated (top panel) and total (bottom panel) (**a**) anti-FOXO3a, (**b**) anti-Akt, and (**c**) anti-IKK-α/β, and (**d**) total PP2A. (**e**) Phosphorylated (top panel) and total (bottom panel) FOXO3a expression in isolated CD8$^+$ memory lymphocytes treated or not with 100 μM OA for 2 h. Results are representative of two to three independent experiments including pooled cells from 8–10 of each genotype per experiment. (**f**) Fold change in Bim mRNA expression in p47$^{phox-/-}$ CD8$^+$ memory lymphocytes treated or not with OA for 4 h. (**g**) Change in non-viable cell count of p47$^{phox-/-}$ CD8$^+$ memory lymphocytes treated or not with OA for 4 h. The data are the mean ($\pm$ S.E.M.) of three separate experiments with pooled cells from 8–10 of each genotype per experiment

p47^{phox} protein and independent of Nox2 enzymatic activity. Consistent with these observations, a recent report by Purushothaman and Sarin showed short hairpin RNA inhibition of gp91^{phox}, but not p47^{phox} inhibited neglect-induced death in activated T cells, and that activated T-cell survival, as well as antigen-specific T-cell persistence and recall, were improved in gp91$^{phox-/-}$ mice following super-antigen challenge.[31] Also consistent with our observations, Richter *et al.*[32] reported that independent of its role in generating Nox2-dependent ROS, p47^{phox} is an important protein for integrating signaling downstream of TLR9 in mouse dendritic cells, thus supporting the idea of distinct and divergent functions for gp91^{phox} and p47^{phox}.

We used flow cytometry to examine CD8$^+$ subsets in the context of *Lm* infection using a previously established classification, which showed antigen-specific memory CD8$^+$ lymphocytes develop rapidly during *Lm* infection.[33] Our results showed considerable differences in antigen-specific Tec, Tem, and Tcm populations in *Lm*-infected p47$^{phox-/-}$ mice relative to similarly infected WT controls. Noticeably, there was an extreme dearth of Tcm but robust CD8$^+$ effector differentiation in *Lm*-infected p47$^{phox-/-}$ spleens following primary and secondary infection. Concurrently, CD8$^+$ T lymphocytes from *Lm*-infected p47$^{phox-/-}$ mice expressed nearly twice as much Bim as WT controls after primary infection. Additionally, although the overall percentage of CD8$^+$ memory lymphocytes were similar in reinfected WT and p47$^{phox-/-}$ spleens the relative ratio of Tem:Tcm were reversed, and Bim expression was significantly higher in p47$^{phox-/-}$ Tcm than WT Tcm. As well, p47$^{phox-/-}$ and WT control Tem:Tcm Bim expression profiles were reversed in the reinfected mice. Although the specific origins of Tem and Tcm are unclear, it has been demonstrated that CD8$^+$ effector and memory cell populations can differentiate from a single naive antigen-specific CD8$^+$ T lymphocyte during *Lm* infection.[33] Therefore, finding that Bim expression is higher in CD8$^+$ memory lymphocytes from *Lm*-infected p47$^{phox-/-}$ mice suggests the observed enhanced Bim expression is related to both cell differentiation and activation. In addition, these findings implicate a role for p47^{phox} in the molecular control of Bim expression in CD8$^+$ memory lymphocytes.

In this study, we successfully propagated CD8$^+$ memory lymphocytes from *Lm*-infected mice and used these *ex vivo* cells to focus on how Bim expression is regulated at the level of transcription in CD8$^+$ memory lymphocyte. Similar to what we observed in *Lm*-infected mice, we found that total CD8$^+$ lymphocyte recovery was significantly less in p47$^{phox-/-}$ CD8$^+$ memory lymphocyte cultures relative to WT cultures, and that the Tem:Tcm ratio was reversed. We also found that CD8$^+$ memory lymphocytes from WT and p47$^{phox-/-}$ cultures expressed Bim transcripts and protein. However, Bim mRNA and protein expression were significantly enhanced in the recovered p47$^{phox-/-}$ CD8$^+$ memory lymphocytes relative to the levels found in similarly treated WT cells. Consistent with finding enhanced Bim transcription in p47$^{phox-/-}$ CD8$^+$ memory lymphocytes, we found that p47$^{phox-/-}$ CD8$^+$ memory lymphocytes express high levels of hypo-phosphorylated FOXO3a protein. Dephosphorylated FOXO3a translocates from the cell cytosol to the nucleus, where it regulates transcription of several genes including pro-apoptotic Bim and FasL transcripts.[24] Thus, FOXO3a is more transcriptionally active in p47$^{phox-/-}$ CD8$^+$ memory lymphocytes.

It has been demonstrated that inhibiting AKT and IKK reduces FOXO3a phosphorylation in CD4$^+$ memory lymphocytes,[8] and that consequently Bim expression was enhanced and apoptosis was induced in the memory lymphocytes.[8] Interestingly, our investigations showed the opposite, that although AKT and IKK were both activated in *ex vivo*-generated p47$^{phox-/-}$ CD8$^+$ memory lymphocytes FOXO3a phosphorylation was reduced. These findings raise additional questions about how FOXO3a is regulated including (1) whether the pro-survival mechanism of the kinases can be redirected toward pro-apoptotic function; and (2) are there other factors that counteract or override the kinase activity? Our investigations revealed data to suggest that another factor, PP2A, may counteract the kinase activity in the absence of p47^{phox}. Specifically, we determined that the Serine/Theronine phosphatase PP2A is abundantly expressed and hyperactive in p47$^{phox-/-}$ CD8$^+$ memory

lymphocytes. We also demonstrated that selectively inhibiting PP2A,[27] enhanced FOXO3a phosphorylation in both p47$^{phox-/-}$ and WT CD8$^+$ memory lymphocytes. Additional investigations are required to tease out the specific mechanisms of how phosphatases, such as PP2A, along with p47^{phox} regulate the post-translational modification of FOXO3a. Both of these questions are the focus of ongoing investigations in our laboratory. Fully active PP2A is a heterotrimeric holoenzyme that consists of a highly conserved catalytic subunit and a scaffolding subunit bound to variable regulatory proteins.[34,35] PP2A is regulated by post-translational modifications including methylation and phosphorylation.[36,37] These investigations revealed that PP2A levels are dramatically high in p47$^{phox-/-}$ CD8$^+$ Tm, and although the relationship between PP2A and p4^{7phox} is not yet defined, our data suggest that p47^{phox} protein can regulate PP2A activity. In addition, it has also been shown that ROS can inhibit PP2A activity and thereby improve cell survival,[38,39] thus implicating a potential role for p47^{phox} in the control of Nox2-independent sources of ROS that may regulate T lymphocyte PP2A activity.

The importance of PP2A for Bim transcription in CD8$^+$ memory lymphocytes was demonstrated by attenuated FOXO3 activation and reduced Bim transcription in p47$^{phox-/-}$ CD8$^+$ memory lymphocytes that were treated with the selective PP2A inhibitor OA,[27] which is an important Serine/Theronine phosphatase in most cells.[34] It has been shown that PP2A dephosphorylates FOXO3a at conserved AKT phosphorylation sites to regulate its subcellular location and transcriptional activity in HeLa cells.[40] In addition, lipoapotosis is mediated by toxic saturated free fatty acids that trigger PP2A activity, which dephosphorylates FOXO3a in hepatocytes.[41] In conclusion, we describe a novel mechanism, which demonstrates that dynamic changes in the phosphorylation state of FOXO3a are not regulated by kinase activity alone, and define a previously unrecognized role for PP2A in the modulation of FOXO3a and CD8$^+$ memory lymphocyte function. Specifically, these findings implicate a role for p47^{phox} protein in the dynamic interplay between PP2A and FOXO3a at the level of pro-apoptotic Bim transcription, where PP2A is a regulatory target of p47^{phox} either directly or through a ROS-dependent mechanism. Further studies will discern the role of p47^{phox} in the kinase–phosphatase balance that regulates FOXO3a and its downstream transcriptional targets in activated CD8$^+$ memory lymphocytes.

Materials and Methods

Mice and bacteria. NADPH oxidase p47^{phox}-deficient (p47$^{phox-/-}$) mice have been described.[15] Backcrossing 14 generations with WT C57BL/6NTac generated congenic p47$^{phox-/-}$ mice on a C57BL/6NTac background. Both congenic p47$^{phox-/-}$ and WT control mice (C57BL/6NTac) were obtained from Taconic Farms, Inc. (Hudson, NY, USA). p47$^{phox-/-}$ were housed in aseptic conditions and given water containing Bactrim (0.13 mg/ml trimethoprim and 0.67 mg/ml sulfamethoxazole (Actiatis MidAtlantic LLC, Columbia, MD, USA). gp91$^{phox-/-}$/Nox2$^{-/-}$ B6.129S6-*Cybb^{tm1Din}*/J mice[17] were obtained from The Jackson Laboratory (Bar Harbor, ME, USA). This study, permit number ASP LHD 11, was reviewed and approved by the Animal Care and Use Committee of the National Institute of Allergy and Infectious Disease of the National Institutes of Health (Public Health Service Assurance A4149-01). The study was carried out in strict accordance with the recommendations in the Guide for the Care and Use of Laboratory Animals of the National Institutes of Health/National Institute of Allergy and Infectious Diseases.

Recombinant *Lm* (r*LM*-OVA,[16]) was a generous gift from Dr. H Shen (University of Pennsylvania, School of Medicine, Philadelphia, PA, USA). The strain was maintained as $-80\,^{\circ}C$ stock in brain–heart infusion (BHI, BD, Sparks, MD, USA)/50% glycerol. Before experimental use, r*LM*-OVA were streaked onto BHI agar. A single colony was inoculated into BHI (BD), and the culture was grown overnight at 37 °C with aeration. The samples were stored in $-80\,^{\circ}C$ in BHI (BD)/50% glycerol. CFU were determined by plating 10-fold serials dilutions of the stock.

Infection of mice and determination of bacterial load. Overnight cultures were serially diluted in PBS to the desired dose and injected into the lateral tail vein of mice. Inocula were plated to verify dose. Mice were infected with 5×10^4 CFU (0.1 LD_{50}) for primary infections. Bacterial loads were determined by plating 10-fold serial dilutions of spleen homogenates in sterile 1% Triton X-100/PBS (Sigma Aldrich, Saint Louis, MO, USA) on BHI agar (BD).

Intracellular stain and flow cytometric analysis. Spleens from mice infected with 5×10^4 CFU of rLM-OVA were aseptically removed and pass though a nylon mesh screen. Red blood cells were lysed with ACK lysing medium (Lonza, Walkersville, MD, USA). Splenocytes (5×10^6 cells/ml) were resuspended in IMDM complete: IMDM (Gibco/Invitrogen Corp., Carlsbad, CA, USA) containing 10% FBS (Hyclone Laboratories, Logan, UT, USA), 2.0 mM L-glutamine (Hyclone), 50 μM β-mercaptoethanol (Sigma Aldrich), and 100 units/ml of penicillin and streptomycin 10 units/Ml (Gibco/Invitrogen Corp.), and incubated with 1 μM of the CD8 or CD4 lymphocyte epitope from ovalbumin, $OVA_{257-264}$ or $OVA_{323-339}$, respectively. $OVA_{257-264}$ and $OVA_{323-339}$ peptides were synthesized by NIAID Research Technologies Branch-Peptide Synthesis and Analysis Unit (Bethesda, MD, USA). One μg/ml Golgistop (BD Biosciences, San Jose, CA, USA) was added for the final 2 h of culture. After 5 h, cells were stained with fluorochrome-labeled antibodies (anti-CD4, -CD8, -CD127, –CD62L and IFNγ) from BD Biosciences and eBioscience, San Diego, CA, USA) using the Cytofix/Cytoperm Kit (BD Biosciences) according to the manufacturer's instructions. For detection of OVA-expressing cells, splenocytes were stained using the iTAg MHC Class I Murine tetramer for $OVA_{257-264}$ (No. T20214, Beckman Coulter, Skyesville, MD, USA) according to the manufacturer's instructions, and cell surface markers (anti-CD4, -CD8, -CD127, and –CD62L from BD Biosciences, eBioscience). For detection of intracellular Bim, splenocytes were washed, fixed, and permeabilized by using the Cytofix/Cytoperm Kit (BD Pharmingen, San Diego, CA, USA) according to the manufacturer's instructions, then incubated with 1 μg anti-Bim_{short} Rat monoclonal (Millipore, Ashland, OR, USA) for 30 min at 4 °C. Anti-Bim was detected with anti-Rat-FITC (BD Biosciences; 30 min at room temperature). Splenocytes were analyzed on a FACS Canto (BD Biosciences), and data were analyzed using FlowJo (Tree Star, Ashland, OR, USA).

***In vitro* CD8$^+$ T lymphocyte killing assay.** The effector CD8$^+$ T lymphocytes from mice infected with 5×10^4 CFU *rLm-OVA* for 7 days were purified (>95% purity) by negative selection using CD8a$^+$ T-cell isolation kit (Milternyi Biotec, Auburn, CA, USA) from splenocytes. The killing assay was performed by co-culturing CD8$^+$ lymphocytes with CFSE-labeled control EL4 cells (ATCC, Manassas, VA, USA) or the OVA-expressing EL4 derivative cell line E.G7-OVA (ATCC) at the indicated effect: target cells ratios. The co-cultures were incubation at 37 °C, and after 4 h the cells were stained by propidium iodide (PI, BD Biosciences). Flow cytometric analysis of PI staining of the CSFE-labeled E.G7-OVA or EL4 target cells was used to determine killing using a FACS Canto (BD Biosciences). Data were analyzed using FlowJo (Tree Star). The results were presented as percentage of PI$^+$ E.G7-OVA or EL4 target cells.

***In vitro* memory CD8$^+$ T-cells generation.** Splenocytes (5×10^6 cells/ml) from mice infected with 5×10^4 CFU of *rLm-OVA* were stimulated with 1 μM $OVA_{257-264}$ peptides (synthesized by NIAID, Bethesda, MD, USA), for 2 days in RPMI 1640 supplemented with 10%FBS. On day 3, CD8$^+$ T lymphocytes were isolated by negative selection using CD8a$^+$ T-cell isolation kit (Milternyi Biotec) according to the manufacturer's instructions.

PP2A inhibition. To pharmacologically inhibit protein phosphatase 2, CD8$^+$ memory T lymphocytes were treated with 50–100 μM OA (Calbiochem, San Diego, CA, USA), as indicated at 37 °C in complete IMDM.

Immunoblotting. *In vitro*-generated memory CD8+ T-cell lysates were prepared in M-PER Buffer (Pierce Biotechnology, Rockford, IL, USA)

supplemented with Halt Protease Inhibitor Cocktail and Phosphatase Inhibitor Cocktail (Pierce Biotechnology). The protein concentrations were determined by the Bradford assay (Pierce Biotechnology). Proteins were resolved by NuPage4-12% Bis-Tris Gel (Invitrogen Corp.) and were transferred to nitrocellulose membranes by iBlot Gel Transfer (Invitrogen Corp.). Immunoblotting analyses were performed by SNAPid system. Immunoblotting analyses were performed by SNAPid system (Millipore, Billerica, MA, USA). Immunocomplexes were reacted with Western Blotting Reaction Reagent (GE Healthcare, Piscataway, NJ, USA). Proteins were visualized by exposure using HyBlot CL film (Denville Scientifics, Metuchen, NJ, USA). Anti-β-actin (Sigma Aldrich), anti-Bim, anti-Akt and anti-phospho-Akt (Ser473), anti-IKKβ and anti-phospho-IKKβ (Ser176/180), anti-Erk and anti-phospho-Erk (Thr202/Tyr204), anti-FOXO3a and anti-phospho-FOXO3a (Ser318/321) (Cell Signaling, Darvers, MA, USA), and anti-PP2A Catalytic a (BD Biosciences) were used as primary antibodies. The secondary antibodies, ECL Rabbit IgG, and HRP-Linked Whole antibody (from goat) were purchased from GE Healthcare.

Quantitative real-time PCR

Total RNA was extracted by using the RNeasy Mini Kit (Qiagen, Valencia, CA, USA) according to the manufacturer's instructions. Quantitative real-time PCR was performed with the 7500 Real Time PCR System (Applied Biosystems, Foster City, CA, USA) and carried out with 1 ng RNA samples and specific Gene Expression Assay (Applied Biosystems) using the TaqMan RNA-to-CT 1-Step Kit (Applied Biosystems). To determine the relative expression, three popular internal controls (GAPDH, PKG1, and RPS29) were tested across all the experimental conditions. RPS29 was chosen to normalize the relative quantification. The Gene Expression Assays for Bim, PUMA, FOXO3a, GAPDH, PKG1, and RPS1 were purchased from Applied Biosystems.

Statistical analysis. Means and S.E.M. were determined. Differences between the two genotype (WT *versus* $p47^{phox-/-}$) group means were analyzed by the Student's *t* test. Multi-group test analysis using repeated measures ANOVA with a Bonferroni post-test using a 0.001 alpha for the 99.9% confidence interval was performed for the *ex vivo* three genotype comparisons of lymphocyte percentages. Differences between mice in the survival analyses were determined by Mantel–Cox log-rank test and the log-rank test for trends (Prism 5, GraphPad Software, Inc., San Diego, CA, USA).

Conflict of Interest

The authors declare no conflict of interest.

Acknowledgements. We thank Kevin Gardner for helpful discussions and critique of this manuscript. We also thank Thomas Leto, Jonathan Yewdell, and Jason Brenchley for careful review and critique of this manuscript. This research was supported by the Division of Intramural Research of the National Institutes of Health/National Institute of Allergy and Infectious Diseases. This was also partially supported by the National Institutes of Health/ National Institute on Minority Health and Health Disparities.

Author Contributions

YL, QL, SS-A, AW, NZ, and SMK performed experiments; SMK managed animal colony; YL, QL, and SHJ analyzed the data; SHJ designed research and wrote the paper.

1. Busch DH, Pilip IM, Vijh S, Pamer EG. Coordinate regulation of complex T cell populations responding to bacterial infection. *Immunity* 1998; **8**: 353–362.
2. Sallusto F, Lenig D, Forster R, Lipp M, Lanzavecchia A. Two subsets of memory T lymphocytes with distinct homing potentials and effector functions. *Nature* 1999; **401**: 708–712.
3. Hand TW, Kaech SM. Intrinsic and extrinsic control of effector T cell survival and memory T cell development. *Immunol Res* 2009; **45**: 46–61.
4. Kurtulus S, Tripathi P, Opferman JT, Hildeman DA. Contracting the 'mus cells'–does down-sizing suit us for diving into the memory pool? *Immunol Rev* 2010; **236**: 54–67.
5. Zhu Y, Swanson BJ, Wang M, Hildeman DA, Schaefer BC, Liu X *et al.* Constitutive association of the proapoptotic protein Bim with Bcl-2-related proteins on mitochondria in T cells. *Proc Natl Acad Sci USA* 2004; **101**: 7681–7686.
6. Hildeman D, Jorgensen T, Kappler J, Marrack P. Apoptosis and the homeostatic control of immune responses. *Curr Opin Immunol* 2007; **19**: 516–521.
7. Sabbagh L, Srokowski CC, Pulle G, Snell LM, Sedgmen BJ, Liu Y *et al.* A critical role for TNF receptor-associated factor 1 and Bim down-regulation in CD8 memory T cell survival. *Proc Natl Acad Sci USA* 2006; **103**: 18703–18708.
8. Riou C, Yassine-Diab B, Van grevenynghe J, Somogyi R, Greller LD, Gagnon D *et al.* Convergence of TCR and cytokine signaling leads to FOXO3a phosphorylation and drives the survival of CD4 + central memory T cells. *J Exp Med* 2007; **204**: 79–91.
9. El-Benna J, Dang PM, Gougerot-Pocidalo MA, Marie JC, Braut-Boucher F. p47phox, the phagocyte NADPH oxidase/NOX2 organizer: structure, phosphorylation and implication in diseases. *Exp Mol Med* 2009; **41**: 217–225.
10. Heyworth PG, Cross AR, Curnutte JT. Chronic granulomatous disease. *Curr Opin Immunol* 2003; **15**: 578–584.
11. Rosenzweig SD. Inflammatory manifestations in chronic granulomatous disease (CGD). *J Clin Immunol* 2008; **28**(Suppl 1): S67–S72.
12. Stasia MJ, Li XJ. Genetics and immunopathology of chronic granulomatous disease. *Semin Immunopathol* 2008; **30**: 209–235.
13. Jackson SH, Devadas S, Kwon J, Pinto LA, Williams MS. T cells express a phagocyte-type NADPH oxidase that is activated after T cell receptor stimulation. *Nat Immunol* 2004; **5**: 818–827.
14. Donaldson M, Antignani A, Milner J, Zhu N, Wood A, Cardwell-Miller L *et al.* p47phox-deficient immune microenvironment signals dysregulate naive T-cell apoptosis. *Cell Death Differ* 2009; **16**: 125–138.
15. Jackson SH, Gallin JI, Holland SM. The p47phox mouse knock-out model of chronic granulomatous disease. *J Exp Med* 1995; **182**: 751–758.
16. Pope C, Kim SK, Marzo A, Masopust D, Williams K, Jiang J *et al.* Organ-specific regulation of the CD8 T cell response to Listeria monocytogenes infection. *J Immunol* 2001; **166**: 3402–3409.
17. Pollock JD, Williams DA, Gifford MA, Li LL, Du X, Fisherman J *et al.* Mouse model of X-linked chronic granulomatous disease, an inherited defect in phagocyte superoxide production. *Nat Genet* 1995; **9**: 202–209.
18. Huster KM, Busch V, Schiemann M, Linkemann K, Kerksiek KM, Wagner H *et al.* Selective expression of IL-7 receptor on memory T cells identifies early CD40L-dependent generation of distinct CD8 + memory T cell subsets. *Proc Natl Acad Sci USA* 2004; **101**: 5610–5615.
19. Huster KM, Stemberger C, Busch DH. Protective immunity towards intracellular pathogens. *Curr Opin Immunol* 2006; **18**: 458–464.
20. Pamer EG. Immune responses to Listeria monocytogenes. *Nat Rev Immunol* 2004; **4**: 812–823.
21. Zenewicz LA, Shen H. Innate and adaptive immune responses to Listeria monocytogenes: a short overview. *Microbes Infect* 2007; **9**: 1208–1215.
22. O'Connor L, Strasser A, O'Reilly LA, Hausmann G, Adams JM, Cory S *et al.* Bim: a novel member of the Bcl-2 family that promotes apoptosis. *EMBO J* 1998; **17**: 384–395.
23. Ley R, Ewings KE, Hadfield K, Howes E, Balmanno K, Cook SJ. Extracellular signal-regulated kinases 1/2 are serum-stimulated 'Bim(EL) kinases' that bind to the BH3-only protein Bim(EL) causing its phosphorylation and turnover. *J Biol Chem* 2004; **279**: 8837–8847.
24. Hedrick SM. The cunning little vixen: Foxo and the cycle of life and death. *Nat Immunol* 2009; **10**: 1057–1063.
25. Hu MC, Lee DF, Xia W, Golfman LS, Ou-Yang F, Yang JY *et al.* IkappaB kinase promotes tumorigenesis through inhibition of forkhead FOXO3a. *Cell* 2004; **117**: 225–237.
26. Medema RH, Kops GJ, Bos JL, Burgering BM. AFX-like Forkhead transcription factors mediate cell-cycle regulation by Ras and PKB through p27kip1. *Nature* 2000; **404**: 782–787.
27. Favre B, Turowski P, Hemmings BA. Differential inhibition and posttranslational modification of protein phosphatase 1 and 2A in MCF7 cells treated with calyculin-A, okadaic acid, and tautomycin. *J Biol Chem* 1997; **272**: 13856–13863.
28. Kurtulus S, Tripathi P, Moreno-Fernandez ME, Sholl A, Katz JD, Grimes HL *et al.* Bcl-2 allows effector and memory CD8 + T cells to tolerate higher expression of Bim. *J Immunol* 2011; **186**: 5729–5737.
29. Endres R, Luz A, Schulze H, Neubauer H, Futterer A, Holland SM *et al.* Listeriosis in p47(phox-/-) and TRp55-/- mice: protection despite absence of ROI and susceptibility despite presence of RNI. *Immunity* 1997; **7**: 419–432.
30. Shiloh MU, MacMicking JD, Nicholson S, Brause JE, Potter S, Marino M *et al.* Phenotype of mice and macrophages deficient in both phagocyte oxidase and inducible nitric oxide synthase. *Immunity* 1999; **10**: 29–38.
31. Purushothaman D, Sarin A. Cytokine-dependent regulation of NADPH oxidase activity and the consequences for activated T cell homeostasis. *J Exp Med* 2009; **206**: 1515–1523.
32. Richter C, Juan MH, Will J, Brandes RP, Kalinke U, Akira S *et al.* Ncf1 provides a reactive oxygen species-independent negative feedback regulation of TLR9-induced IL-12p70 in murine dendritic cells. *J Immunol* 2009; **182**: 4183–4191.
33. Stemberger C, Huster KM, Koffler M, Anderl F, Schiemann M, Wagner H *et al.* A single naive CD8 + T cell precursor can develop into diverse effector and memory subsets. *Immunity* 2007; **27**: 985–997.
34. Virshup DM. Protein phosphatase 2A: a panoply of enzymes. *Curr Opin Cell Biol* 2000; **12**: 180–185.
35. Xu Y, Xing Y, Chen Y, Chao Y, Lin Z, Fan E *et al.* Structure of the protein phosphatase 2A holoenzyme. *Cell* 2006; **127**: 1239–1251.
36. Chen J, Martin BL, Brautigan DL. Regulation of protein serine-threonine phosphatase type-2A by tyrosine phosphorylation. *Science* 1992; **257**: 1261–1264.

37. Tolstykh T, Lee J, Vafai S, Stock JB. Carboxyl methylation regulates phosphoprotein phosphatase 2A by controlling the association of regulatory B subunits. *EMBO J* 2000; **19**: 5682–5691.
38. Chen L, Liu L, Yin J, Luo Y, Huang S. Hydrogen peroxide-induced neuronal apoptosis is associated with inhibition of protein phosphatase 2A and 5, leading to activation of MAPK pathway. *Int J Biochem Cell Biol* 2009; **41**: 1284–1295.
39. Finnegan S, Mackey AM, Cotter TG. A stress survival response in retinal cells mediated through inhibition of the serine/threonine phosphatase PP2A. *Eur J Neurosci* 2010; **32**: 322–334.
40. Singh A, Ye M, Bucur O, Zhu S, Tanya Santos M, Rabinovitz I *et al.* Protein phosphatase 2A reactivates FOXO3a through a dynamic interplay with 14-3-3 and AKT. *Mol Biol Cell* 2010; **21**: 1140–1152.
41. Barreyro FJ, Kobayashi S, Bronk SF, Werneburg NW, Malhi H, Gores GJ. Transcriptional regulation of Bim by FoxO3A mediates hepatocyte lipoapoptosis. *J Biol Chem* 2007; **282**: 27141–27154.

Supplementary Information accompanies the paper on Cell Death and Disease website (http://www.nature.com/cddis)